On the diurnal, weekly, seasonal cycles and annual trends in atmospheric CO_2 at Mount Zugspitze, Germany during 1981–2016

Ye Yuan[1], Ludwig Ries[2], Hannes Petermeier[3], Thomas Trickl[4], Michael Leuchner[1,5], Cédric Couret[2], Ralf Sohmer[2], Frank Meinhardt[6], Annette Menzel[1,7]

5 [1]Department of Ecology and Ecosystem Management, Technical University of Munich (TUM), Freising, Germany
[2]German Environment Agency (UBA), Zugspitze, Germany
[3]Department of Mathematics, Technical University of Munich (TUM), Garching, Germany
[4]Institute of Meteorology and Climate Research, Atmospheric Environmental Research (IMK-IFU), Karlsruhe Institute of Technology (KIT), Garmisch-Partenkirchen, Germany
10 [5]Springer Nature B.V., Dordrecht, Netherlands
[6]German Environment Agency (UBA), Schauinsland, Germany
[7]Institute for Advanced Study, Technical University of Munich (TUM), Garching, Germany

Correspondence to: Ye Yuan (yuan@wzw.tum.de)

Abstract. A continuous, 36-year measurement record of atmospheric carbon dioxide (CO_2) at three measurement sites of

15 Mount Zugspitze, Germany was studied. The CO_2 trend and seasonality were analyzed by decomposing the long-term time series into trend and seasonal components. The mean CO_2 annual growth rate over the 36 year period at Zugspitze is 1.8 ppm yr^{-1}, which is in good agreement with the Mauna Loa station and the global means. The peak-to-trough amplitude of the mean CO_2 seasonal cycle is 11.67 ppm at Mount Zugspitze, which is significantly less than nearby measurement sites at Mount Wank and Schauinsland, but which follow similar patterns. To characterize this mountain site better, analyses of

20 weekly periodicity and the diurnal cycle were performed to provide evidence of local sources and sinks of CO_2. Together, with an atmospheric trace gas (CO and NO) and the number of site visitor case study, clear weekday–weekend differences were detected, indicating potential CO_2 sources in the near vicinity.

1. Introduction

Long-term records of atmospheric carbon dioxide (CO_2) improve our understanding of the global carbon cycle, as well as

25 long- and short-term changes, especially at remote background locations. The longest continuous measurements of atmospheric CO_2 trace back to 1958 at Mauna Loa, Hawaii, taken by the Scripps Institution of Oceanography (Pales and Keeling, 1965). The measurements were performed at long distances from CO_2 sources and sinks, situated on the north slope of the Mauna Loa volcano at an elevation of 3397 m above sea level (a.s.l.). Later, additional measurement sites were established for background studies of global atmospheric CO_2, such as the South Pole (Keeling et al., 1976), Cape Grim,

30 Australia (Beardsmore and Pearman, 1987), Mace Head, Ireland (Bousquet et al., 1996), and Baring Head, New Zealand (Stephens et al., 2013). Apart from the sites located either in the Antarctica or along coastal/island regions, continental mountain stations also offer excellent options to observe the background atmospheric levels due to high elevations that are

least unaffected by local influences, for example, Mount Waliguan, China (Zhang et al., 2013), Mount Cimone, Italy (Ciattaglia, 1983), Jungfraujoch, Switzerland, and Puy de Dôme, France (Sturm et al., 2005). Presently, there are 31 Global Observatories coordinated by the Global Atmosphere Watch (GAW) network, focusing on monitoring the physical and chemical state of the atmosphere on a global scale.

5   Although mountainous sites experience less impact from local pollution and represent an improved approach to background conditions compared with stations at lower elevations, we cannot fully dismiss the influence of local to regional emissions. This influence depends largely on air-mass transport and mixing within the moving boundary layer height. Based on lidar measurements, air, during the daytime, from the boundary layer is orographically lifted to approximately 1–1.5 km above typical summit heights during the warm season (Carnuth and Trickl, 2000; Carnuth et al., 2002). Based on a 14-year record

10 of atmospheric CO_2 at Mount Waliguan (3816 m a.s.l.), China, significant diurnal cycles and depleted CO_2 levels were observed during the summer that are mainly driven by biological and local influences from adjacent regions, although the magnitude and contribution of these influences are smaller than other continental or urban sites (Zhang et al., 2013). At the Mt. Bachelor Observatory (2763 m a.s.l.), U.S.A., atmospheric CO_2 variations were studied in the free troposphere and boundary layer separately, where wildfire emissions were observed to drive CO_2 enhancement at times (McClure et al.,

15 2016). However, it still remains unclear as to exactly what extent that elevated mountain sites are influenced by local activities and how to better characterize local sources and sinks at such sites. It is difficult to make quantitative conclusions on the anthropogenic and biogenic contributions to these measurements (Le Quéré et al., 2009). Analyzing weekly periodicity may be a potential indicator since periodicity represents anthropogenic activity patterns during one week (seven days) without the influence of natural causes (Cerveny and Coakley, 2002). The results from Ueyama and Ando (2016)

20 clearly indicated the presence of elevated weekday CO_2 emissions compared with weekend and/or holiday CO_2 emissions at two urban sites in Sakai, Japan. Cerveny and Coakley (2002) detected significantly lower CO_2 concentrations on weekends than on weekdays at Mauna Loa, which was assumed to result from anthropogenic emissions from Hawaii and nearby sources.

    In this study, we present a continuous, 36-year record of atmospheric CO_2 measurements (1981–2016) at Mount Zugspitze,

25 Germany (2962 m a.s.l.). The objective of this study is to produce a consistent overall analysis of CO_2 trend and seasonality, and an improved measurement site characterization with respect to historical CO_2 data in terms of diurnal and weekly cycles. The CO_2 measurements were performed at three locations on Mount Zugspitze: at a pedestrian tunnel (ZPT), at the summit (ZUG), and at the Schneefernerhaus (ZSF) on the southern face of the mountain. In addition, CO_2 measurements were taken at the nearby lower mountain station, Wank Peak (WNK), but for a shorter time period. The results for the CO_2 annual

30 growth rates and seasonal amplitudes were studied separately via trend-seasonal decomposition and compared with CO_2 data for the comparable time period (1981–2016) at the GAW Regional Observatory Schauinsland, Germany (SSL) and the GAW Global Observatory Mauna Loa, Hawaii (MLO), as well as the global CO_2 means calculated by the NOAA/ESRL and the World Data Centre for Greenhouse Gases (WDCGG). Weekly CO_2 periodicities were evaluated with the diurnal cycles

for the Mount Zugspitze sites. In addition, we perform an atmospheric CO and NO case study together with the amount of passengers at Zugspitze in 2016 as potential indicators for weekday–weekend influences.

2. Experimental methods and data

2.1. Measurement sites

5 Mount Zugspitze is located approximately 90 km southwest of Munich, Germany. The nearest populated city is Garmisch-Partenkirchen (GAP, 708 m a.s.l., see Fig. 1). Measurements of CO_2 were first performed between 1981 and 1997 with different, consecutively used instrument models (i.e., the URAS-2, 2T, and 3G), using nondispersive infrared (NDIR) technique. The measurements were collected at a southward-facing balcony in a pedestrian tunnel (Reiter et al., 1986) from the summit of Mount Zugspitze to the Schneefernerhaus (ZPT, 47°25′ N, 10°59′ E, slightly below the summit), which was a

10 hotel until 1992 when it was rebuilt into an environmental research station. From 1995 until 2001, a new set of measurements began at the summit (ZUG, 47°25′ N, 10°59′ E, 2960 m a.s.l.) at a sheltered laboratory on the terrace using a URAS-3G device. These two measurement periods were performed by the Fraunhofer-Institute for Atmospheric Environment Research (IMK-IFU), and, since 1995 these measurements have been carried out on behalf of the German Environmental Agency (UBA). Since 2001, to continue contributing to the GAW Programme, CO_2 measurements have been

15 performed at the Environmental Research Station Schneefernerhaus (ZSF, 47°25′ N, 10°59′ E, 2656 m a.s.l.). Zugspitzplatt, a glacier plateau approximately 100 m below the Schneefernerhaus can be reached from the valley via cable cars or cogwheel trains. The Zugspitzplatt descends eastward via a moderate to steep slope across the Knorrhütte towards the Reintalangerhütte shown in Fig. 1 (Gantner et al., 2003). Measurements of CO_2 at Schneefernerhaus continued thereafter to the present with a modified HP 6890 by using gas chromatography (GC) method with an intermediate upgrade in 2008

20 (Bader, 2001; Hammer et al., 2008; Müller, 2009). In 2012 and 2013, an instrumental failure occurred, such that measurements of CO_2 required parallel measurements with a cavity ring-down spectrometer (CRDS, Picarro EnviroSense 3000i) connected to the same air inlet.

Additional atmospheric CO_2 measurements throughout the GAP area were performed between 1978 and 1996 at the Wank summit (WNK, 47°31′ N, 11°09′ E, 1780 m a.s.l.) using a URAS-2T instrument. The Wank Observatory is located in alpine

25 grasslands just above the tree line (Reiter et al., 1986; Slemr and Scheel, 1998). A more detailed description can be found in Table 1. Detailed information on the CO_2 measurements at Schauinsland (SSL, 47°55′ N, 7°54′ E, 1205 m a.s.l.) and Mauna Loa, Hawaii (MLO, 19º28′ N, 155º35′ W, 3397 m a.s.l.), which we use to compare with the results of this study, can be found in Schmidt et al. (2003) for SSL and Thoning et al. (1989) for MLO.

2.2. Data processing

30 CO_2 mole fractions were processed separately because of different measurement sites and time periods at Mount Zugspitze as described above. Information for the first and second time periods were mainly collected based on personal

communication with corresponding staff and logbooks. The data calibration and filtering procedures described in detail focus on CO_2 measurement performed at ZSF.

At ZSF, calibrations were carried out at 15 minute intervals using working standards, which had been calibrated with station standards from the GAW Central Calibration Laboratory (CCL) operated by the NOAA/ESRL Global Monitoring Division. The GC data acquisition system (see Supplementary Fig. S1) produced a calibration value every 15 minutes and two values from the sampled air based on one chromatogram every five minutes. Calibration factors and metadata were used to convert raw data into the final data product. Invalid and unrepresentative data due to local influences were flagged according to a pollution list. The measurement quality was controlled by comparison with simultaneous measurements of identical gas or with measurements of other trace substances and meteorological data, and additional support from station logbooks and checklists. The data were flagged according to quality control results. In principle, the acquisition system stores all measured data (flagged or not) and never discards them. Drifts in the working standards were controlled by a quasi-continuously measured second target and a regular two-month inter-comparison between the working standard and NOAA station standards, performing corrections as needed. Averaged 30-min values were generated by calculating the arithmetic mean of the remaining data with a minimum of 2/3 of all the data.

2.3. Offset adjustment

According to the NOAA CMDL (http://ds.data.jma.go.jp/wcc/co2/co2_scale.html), no significant offsets are documented between the calibration scales WMO X74 and WMO X85 and the current WMO mole fraction scale. However, for the three-year parallel CO_2 measurements at ZPT and ZUG (1995–1997), we observe significant offsets ($CO_{2, ZUG}$ minus $CO_{2, ZPT}$, detailed offset plots can be found in Supplementary Fig. S2). We assume that this offset exists due to pressure broadening effects on the analyzers. As Table 1 shows, different calibration gases were used at ZPT (CO_2 in N_2) and ZUG (CO_2 in natural gas). However, due to a lack of information, a potential offset adjustment for further analyses was made to the ZPT CO_2 record based on differences in the overlapping years. For the adjustment, we used the mean offset from these three years (5.802 ± 0.004 ppm) and added this to the ZPT data. The data measured at WNK were also calibrated similarly based on the same X74 scale used at ZPT as well as using CO_2 in N_2 gases, such that an identical value was added to the WNK data. Nevertheless, the results of this study still need to be viewed with caution, especially for the ZPT historical data and parameters such as the annual growth rates. Various analyzers were used during different periods, which could potentially cause variations as well as uncertainty in the offset adjustment.

On the other hand, there were 9 consecutive months, from April to December 2001, of parallel atmospheric CO_2 measurements at both ZUG and ZSF, based on which an inter-comparison between the two series was made. The mean offset between the two records attained an average of -0.11 ± 0.03 ppm ($CO_{2, ZSF}$ minus $CO_{2, ZUG}$), which is still in good agreement between ZUG and ZSF with respective to the GAW Data Quality Objective (DQO, ± 0.1 ppm) for atmospheric CO_2 in the Northern Hemisphere.

In this study, CO_2 time series analyses for Mount Zugspitze sites are organized in the following ways. We took measurements during the corresponding time intervals at ZPT (1981–1994), ZUG (1995–2001), and ZSF (2002–2016) to assemble a full 36 year time series. For site characterization, we treat each site separately with respect to weekly and diurnal analyses. At WNK, we used measured CO_2 data between 1981 and 1996 (for consistency with Zugspitze, which began in

5   1981).

2.4. ADVS data selection

Adaptive Diurnal minimum Variation Selection (ADVS), a novel statistical data selection strategy, was used to ensure that the data were clean and consistent with respect to the state of locally unaffected lower free troposphere at the measurement sites (Yuan et al., 2018). ADVS, which was originally designed to characterize mountainous sites, selects data based on

10   diurnal patterns with the aim of selecting optimal data that can be considered representative of the lower free troposphere. To achieve this, variations in the mean diurnal CO_2 were first evaluated and a time window was selected based on minimal data variability around midnight, at which point data selection began. The data outside the starting time window were examined on a daily basis both forwards and backwards in time for the day under consideration by applying an adaptive threshold criterion. The selected data results represent background CO_2 levels at the different measurement sites.

15   ADVS data selection was applied to all CO_2 records, followed by the calculation of the percentages of the ADVS-selected data. Figure 2 shows the CO_2 time series before and after ADVS data selection. The percentages of ADVS-selected data are 3.7% for SSL, 6.5% for WNK, 13.5% for Zugspitze, and 37.9% for MLO. Lower percentages indicate higher data variability due to lower elevation and proximity to local sources and sinks.

2.5. STL decomposition

20   The Seasonal-Trend Decomposition technique (STL) was applied to decompose the CO_2 time series into trend, seasonal and remainder components individually (Cleveland et al., 1983; Cleveland et al., 1990), which, in previous studies, has been a commonly applied method (Stephens et al., 2013; Hernández-Paniagua et al., 2015). Locally weighted polynomial regressions were iteratively fitted to all monthly values in both an outer and an inner loop. According to Cleveland et al. (1990) and Pickers and Manning (2015), we set the trend and seasonal smoothing parameters to 25 and 5, respectively. The

25   CO_2 time series at each site were aggregated into monthly averages and, then, decomposed by STL. Missing monthly values were substituted by spline interpolation.

To study the trend and seasonality, we intended to apply STL decomposition to the ADVS-selected time series. However, due to multiple occurrences of consecutively missing values in the ADVS-selected monthly averages, especially for measurement sites at lower elevations, we found that it was more practical to use the original CO_2 time series without ADVS

30   data selection for STL decomposition, to preserve time series continuity (Pickers and Manning, 2015). Nevertheless, there is one missing six-month time interval at Zugspitze in 1998 (July to December). Thus, for Zugspitze, STL was performed

separately for the time periods before (1981.01–1998.06) and after (1999.01–2016.12), and the decomposed results were combined afterwards (see Supplementary Fig. S3).

For annual growth rates, we did not include the WNK time series due to shorter time periods of available data. Monthly trend components were first aggregated into annual mean values. Then, the annual CO_2 growth rates were calculated as the

5   difference between the CO_2 value of the current year and the value from the previous year (Jones and Cox, 2005). The mean seasonal cycle was aggregated directly from the monthly seasonal components by month. To observe potential deviations on the regional and global scale, we compared the trend and seasonality derived from the STL decomposed components respectively at Zugspitze with other measurement sites. We included the globally averaged marine surface monthly mean data from the NOAA (www.esrl.noaa.gov/gmd/ccgg/trends/) and data for the global mean mole fractions from the WDCGG

10   (WMO, 2017) as references and processed based on the identical STL decomposition routine.

2.6. Mean Symmetrized Residual

Weekly periodicity significance was calculated using the "Mean Symmetrized Residual" (MSR), which was originally applied to atmospheric CO_2 data (Cerveny and Coakley, 2002). In doing so, we were cautious when choosing the most appropriate statistical analysis (Daniel et al., 2012; Sanchez-Lorenzo et al., 2012). The MSR method focuses on variations in

15   mean values by the days of the week. Daily deviations from the seven-day (consecutive) averages are calculated to account for the most likely emission cycles. Then, the MSR values are derived by averaging the differences for each single day. Additionally, only the MSR values with no data gaps in all the seven differences are considered as valid. Finally, all the MSR values are aggregated into overall mean values for each day of the week. In addition, a standardized adjustment is also done so that the sum of all the seven values is equal to 0 (Cerveny and Coakley, 2002). All the statistical analyses described

20   above (including STL, ADVS, and MSR) were performed in the R environment (R Core Team, 2018).

3. Results and discussion

3.1. Trend and seasonality

Based on the STL decomposed results, the mean annual growth rate over the entire 36 year period at Mount Zugspitze is 1.78 ± 0.34 ppm yr^{-1}, which is consistent with the SSL (1.84 ± 0.39 ppm yr^{-1}), MLO (1.82 ± 0.21 ppm yr^{-1}), and global

25   means (NOAA: 1.79 ± 0.21 ppm yr^{-1}; WDCGG: 1.84 ± 0.20 ppm yr^{-1}). In general, the mean annual growth rates over the entire 36 year period at all sites agree within a range of 1.8 ppm yr^{-1}. Then, we divided the entire time period (1981–2016) into three time blocks, i.e., ZPT, ZUG, and ZSF, to calculate the mean annual CO_2 growth rates to observe potential differences with other sites (see Table 2). The mean annual growth rates at all Zugspitze sites agree with those for the other sites, which in general, show clear, increasing trend over the time blocks. Only the mean annual growth rate between 1995

30   and 2001 at the ZUG site is much lower than the other sites due to missing values in 1998 so that the annual growth rates for

1997 and 1998 are left out. Möller (2017) also mentioned that growth rates at both German stations and the MLO from 1981 to 1992 were identical.

For the overall seasonality, Figure 3a presents the mean seasonal cycles for the STL decomposed seasonal components. We observed similar patterns in the SSL and WNK seasonal cycles, with mean peak-to-trough amplitudes of 15.44 and 14.89 ppm, respectively. The Zugspitze sites have a lower amplitude (11.67 ppm), but also have a similar seasonality influenced by active biogenic processes (mainly photosynthesis) during the summer (seasonal minima in August) compared with the SSL and WNK (Dettinger and Ghil, 1998). As vegetation grows with rising temperatures (approaching summer), CO_2 levels decrease due to more and more intense photosynthetic activities that minimize in August. In addition, with rising temperatures, locally influenced air masses reach the Zugspitze sites more often due to "alpine pumping" (Carnuth et al., 2002; Winkler et al., 2006). Sampled air is more frequently mixed with air from lower levels, which is characterized by lower CO_2 concentrations that also minimize in August. Anthropogenic activities and plant respiration dominate the increases in concentration in the winter (January to April). This influence appears to be stronger at SSL and WNK than at the elevated Zugspitze site. Lower levels of CO_2 and a one-month delay, from February to March, for the seasonal maximum at Zugspitze are in agreement with the expectation of thermally driven orographic processes that drive the upward transport of CO_2 from local sources, as well as limited human access to the Zugspitze site and the almost non-existent presence of biogenic activities at such high elevations.

The MLO is characterized by a seasonal maximum in May and a minimum in September with a peak-to-trough amplitude of 6.73 ppm, which agree with observations from Dettinger and Ghil (1998) and Lintner et al. (2006). Moreover, global means exhibited the lowest seasonal amplitudes of 4.33 ppm (NOAA) and 4.76 ppm (WDCGG). The NOAA global mean fits better towards the MLO seasonal cycle, compared with the WDCGG, indicating the presence of a typical Marine Boundary Layer (MBL) condition for the levels of background CO_2 in the atmosphere. The WDCGG global mean includes continental characteristics and, thus, exhibits a slightly more continental signature, seen from the seasonal cycles for the continental sites, such as at Zugspitze.

We separately examine, in more detail, the seasonal cycles at ZPT, ZUG, and ZSF (see Fig. 3b). Despite the close proximity, there are slight differences in seasonal amplitudes (ZPT: 10.86 ppm; ZUG: 11.14 ppm; ZSF: 13.09 ppm) among the three sites. Figure 3b shows good agreement between CO_2 concentrations from April to June and from October to December. Apart from this, significantly higher levels of CO_2 at ZSF from January to March and lower levels from July to September cannot be neglected. Similarly, as Fig. 3a shows, these results indicate that factors such as elevation and site surroundings have a strong influence on determining the air-mass composition in view of local, vertical transport. The amount of air-mass transport via orographic lifting affects the three sites differently. The lower elevation station, ZSF, apparently captures more mixed air masses when measuring CO_2 levels, which follows a daytime up-valley flow along the Reintal, as well as a slightly southeastern flow from Inntal that reaches the ZSF site (see Fig. 1) that is less frequent for higher elevation sites (ZPT or ZUG). In addition, comparably postponed seasonal maxima at ZUG and ZPT from March to April show delayed onset of convective upwind air-mass transport and changing Planetary Boundary Layer (PBL) compositions.

3.2. Inter-annual variation

To study the inter-annual variability, we focused on the percentages of ADVS selection, the growth rates, and the seasonal amplitudes annually. The annual percentages from ADVS data selection are shown for years without missing monthly averages (see Fig. 4a). Therefore, 1982, 1994, and 1998 for the Zugspitze sites, 1996 for WNK, and 1981, 1982, 2010, 2011,

5   and 2014 for SSL were excluded. An abnormally high percentage at Zugspitze in 2000 resulted from careful and intensive filtering of the original CO_2 data. The total number of validated 30-min data points in 2000 is 4634, while the amount of data for other years is approximately 15000. As described in the previous section, the mean annual growth rates are plotted in Fig. 4b. The annual CO_2 seasonal amplitudes are calculated as the difference between the yearly maximum and minimum monthly CO_2 values from the STL decomposed seasonal components (see Fig. 4c).

10 Focusing on the annual percentages from ADVS-selected representative data after 1990, we calculated the mean annual percentages at the Zugspitze sites, for the time periods between 1990 and 2001, and 2002 and 2016. We observe significantly higher percentages at a 95% confidence interval, at ZPT and ZUG ($20.59 \pm 4.12\%$) compared with values at ZSF ($13.63 \pm 1.10\%$), which are different from the SSL (4.20 ± 0.53 vs. $4.20 \pm 0.58\%$) and the MLO (41.10 ± 1.42 vs. $38.42 \pm 1.87\%$). A likely explanation is there are systematically different air-mass transport characteristics reaching each of these sites. Higher

15 percentages at ZPT and ZUG indicate that these sites are capable of capturing more air masses that have traveled over long distances along the mountains. These air masses trap air that ascends from many Alpine valleys, but also from remote source regions up to intercontinental scale (Trickl et al., 2003; Huntrieser et al., 2005). On the other hand, the ZSF is dominated by mixing air masses that have traveled along the Zugspitzplatt area, which contain higher levels of CO_2 due to daily, local anthropogenic sources during winter and convective upwind during seasons without snow cover that are characterized by

20 lower concentrations of CO_2 at lower altitudes. Such patterns in the data can also be illustrated for the annual growth rates and seasonal amplitudes. The overall patterns at the Zugspitze sites agree with the SSL and WNK. However, the SSL and WNK exhibit much more variation in the annual growth rates and higher seasonal amplitude levels (see Fig. 4b and 4c). In addition, slightly higher seasonal amplitudes for the WDCGG global mean compared with the NOAA one can be explained by the WDCGG global mean calculation methods, which includes more continental stations (WMO, 2017).

25 Anomalies in the annual growth rates are frequently observed, which are possibly explained by climatic influences such as the El Nino-Southern Oscillation (ENSO), volcanic activity, and extreme weather conditions (Keeling et al., 1995; Jones and Cox, 2001; Francey et al., 2010; Keenan et al., 2016). One of the largest positive annual growth rate anomalies occurs in 1998 and is clearly seen in all the records (aside from the WNK and Zugspitze sites that have missing values), which is attributed to a strong El Niño event (Watanabe et al., 2000; Jones and Cox, 2005). Similar signals are found in 1988,

30 especially at the MLO and in the global means. Such anomalies are more clearly observed in the global and seaside time series. Regarding continental sites, inter-annual signals may be hidden by more intense land influences rather than global effects. Moreover, positive consecutive anomalies between 2002 and 2003 are clearly observed at Zugspitze and the SSL, which are potentially due to anomalous climatic conditions, such as the dry European summer in 2003 that led to an increasd

number of forest fires. These events are also observable in the MLO and global mean records but at smaller scales (Jones and Cox, 2005). At all German sites, clear negative anomalies, due to violent eruptions of the El Chichón and Mt. Pinatubo volcanoes and the subsequent volcanic induced surface cooling effect, are observed after stratospheric aerosol maxima above Garmisch-Partenkirchen in 1983 and 1992, respectively (Lucht et al., 2002; Frölicher et al., 2011; Frölicher et al., 2013;

5 Trickl et al., 2013). This effect is only slightly visible in the MLO and global mean records despite the fact that volcanic aerosol spread over the entire globe.

However, the reasons for some anomalies are still unclear. These include the negative anomalies during 1985 and 1986 at all Germans sites. Certain anomalies in the annual percentages and seasonal amplitudes also derive from extremely low ADVS selection percentages beginning at 1984 and continuing until 1990, with peaks in seasonal amplitudes between 1985 and

10 1986. This is the reason why we calculated the mean annual ADVS selection percentage beginning at 1990. We assume that similar physical mechanisms between sites do not occur due to local influences. However, annual percentages at the MLO also have similar characteristics. Therefore, it is still unclear what triggers such distinct inter-annual data variability across measurement sites. Another clear negative annual growth rate anomaly occurred in 2014 across all sites. Such anomalies still require further investigation but are beyond the scope of this study.

15 **3.3. Weekly periodicity and diurnal variation**

To characterize site differences at Mount Zugspitze better, we analyzed the mean CO_2 weekly cycles as a function of mean MSR values (see Fig. 5a). The mean MSR values at the MLO for the corresponding time intervals were also calculated. Most weekly cycles exhibit no clear peaks or troughs patterns for both sites. However the magnitude of MSR data variability is much higher at Zugspitze with a maximum on Thursdays for several periods. The only weekday–weekend pattern is

20 observed at ZSF, which shows weekly maxima and weekly minima on Thursday and Saturday, respectively (peak-to-trough difference: 0.76 ppm), significantly different at the 95% confidence interval. Gilge et al. (2010) observed similar phenomena when studying O_3 and NO_2 concentrations at Alpine mountain stations including Zugspitze. Clear weekly cycles, with enhanced O_3 levels on working days, were observed at ZSF in summer, with weekly maxima and minima on Thursday and Sunday, respectively. For NO_2, they continually observed maximum mixing ratios on work days and minimum ratios on

25 Sundays at neighboring stations, generally suggesting that there is an anthropogenic impact at all elevations.

We obtained more insights into the weekly Zugspitze CO_2 cycle by comparing the mean diurnal cycles between weekdays and weekends (see Fig. 5b). Detrended mean diurnal cycles at ZSF, from Sunday to Saturday, were calculated by subtracting the daily averages from the daily data between 2002 and 2016. Morning CO_2 levels at ZSF (i.e., weekday peaks at around 9–10 a.m. LT) are higher on weekdays than weekends, while CO_2 levels during the rest of the week are relatively stable. Such

30 weekly cycles are not observable at other Zugspitze sites, or at the WNK and SSL (see Supplementary Fig. S4). At ZPT, there is nearly no diurnal variation, indicating that this site has the closet characteristics to background conditions. The weekday–weekend differences at ZSF are possibly due to local working patterns, whereas the absence of this pattern at

lower sites may indicate influences from a more regional reservoir. In fact, this measurement site is closed on the weekends and, thus, influenced by less anthropogenic activities.

3.4. Case study with atmospheric CO, NO, and the number of daily passengers at Zugspitze

To further study the potential sources and sinks for such weekday–weekend differences in the CO_2 diurnal cycles at ZSF, we analyzed atmospheric CO and NO data at ZSF and the daily, combined number of passengers from Zugspitzplatt and the summit of Zugspitze during 2016. Atmospheric CO and NO are known to be good indicators of local anthropogenic influences due to highly variable short-term signals and, thus, are helpful when attempting to identify potential CO_2 sources (Tsutsumi et al., 2006; Sirignano et al., 2010; Wang et al., 2010; Liu et al., 2016). In this study, we used atmospheric NO due to its short lifetime based on rapid atmospheric NO_2 formation with adjacent altitudinal dependent O_3 surplus, indicating the presence of sources at closer distances. The CO and NO data shown in Fig. 6 for the mean weekly cycle include data that was flagged during data processing, because for the delivery to GAW world data centers the logged and recognized work dependent concentration peaks are flagged. A clear weekday–weekend difference is observed for both CO and NO. Only weekdays are characterized by multiple short-term atmospheric CO events and higher atmospheric NO peaks during the daytime (mostly around 9 a.m. LT), which fits perfectly with daytime peaks in CO_2 diurnal cycles. A general increasing and decreasing pattern in NO throughout the week is thought to originate from heating at Zugspitzplatt and work with combustion engines. On the other hand, the daily number of passengers at Zugspitze (see Fig. 6c) shows a clear weekday–weekend pattern, as well as with the higher number of passengers on the weekends. However, increased numbers of passengers on the weekends do not correspond to higher levels of CO and CO_2, indicating that measured CO_2 levels are not significantly influenced by tourist activities at nearby sites. Instead, it is more likely that anthropogenic working activities are the main driver of weekly periodicity.

4. Conclusions

In this study, we presented a time series analysis of a 36-year CO_2 measurement record at Mount Zugspitze in Germany together with a thorough study of the weekly periodicity combined with diurnal cycles. Even though it is challenging to quantify local sources and sinks, this study shows that it is possible to gain information on variation in this regard. Compared with the GAW Regional Observatories at Schauinsland and Wank Peak, as well as the GAW Global Observatory at Mauna Loa, Zugspitze proves to be a highly suitable site for monitoring background levels of air components with proper data selection procedures. Long-term trend at Zugspitze agrees with Mauna Loa and global means, while seasonality and short-term variations show similar patterns but are considerably less influenced by local to regional mechanisms than lower elevation stations at Schauinsland and Wank Peak. Inter-annual variations also correlate well with anomalous global events. However, several anomalies still exist across most stations that lack clear explanations. These anomalies require further investigation possibly by analyzing correlations between extreme events and historical meteorological or hydrological data.

Finally, we observe that, at Zugspitze, we cannot neglect local to regional influences. Seasonal amplitude at Zugspitze is significantly more influenced by biogenic activity, mostly in the summer, at regional sites compared with global sites. On the other hand, weekly periodicity analysis provides a clear picture of local CO_2 sources that potentially result from human working activities, especially at ZSF. Overall, this study provides detailed insights into long-term atmospheric CO_2

5   measurements, as well as site characteristics at Mount Zugspitze. We propose the application of this type of analysis as a systematic tool for the physical and quantitative classification of stations with respect to their lower free tropospheric representativeness. As an additional component in this analysis, weekly periodicity can be used to analyze anthropogenic influences. The systematic application of this approach to larger continental or global regions can serve as a basis for more quantitative analyses of global greenhouse gases trends such as CO_2. Based on the physical foundation of the methodology

10   presented here, we suggest that these techniques can be applied to other greenhouse gases such as SF_6, CH_4, and aerosols.

Acknowledgements

This study was supported by a scholarship from the China Scholarship Council (CSC) under Grant CSC No. 201508080110. Our thanks go to the support from a MICMoR Fellowship through the KIT/IMK-IFU to Ye Yuan. Our thanks go to Gourav Misra for the geographical map of the measurement sites. Our thanks go to James Butler and Kirk Thoning from NOAA for

15   their indispensable discussions on the problematic nature of representing and comparing data on different older and actual CO_2 scales. The CO_2, CO and NO measurements at Zugspitze Schneefernerhaus, Platform Zugspitze of the GAW Global Observatory Zugspitze/Hohenpeissenberg, and CO_2 measurements at Schauinsland are supported by the German Environment Agency (UBA). The INK-IFU provided data from the Zugspitze tunnel and summit. Our thanks go to Dr. H. E. Scheel from the IMK-IFU for his high quality data measurement until 2001 at the Zugspitze Summit (ZUG). During a long

20   period, Dr. Scheel, who passed away in 2013, led the in-situ measurement program at the Zugspitze summit with a high level of expertise and diligence. We would also like to thank the operating team at the Environmental Research Station Schneefernerhaus for supporting our scientific activities and to the Bavarian Ministry for Environment for supporting this High Altitude Research Station. Finally, our gratitude goes to the Bavarian Zugspitze Railway Company for the passenger data in 2016.

25   **Data availability**

NOAA global mean: ftp://aftp.cmdl.noaa.gov/products/trends/co2/co2_mm_gl.txt.
WDCGG global mean: https://ds.data.jma.go.jp/gmd/wdcgg/pub/global/2017/co2_monthly_20171030.csv.
CO_2 records (also including CO and NO) of all GAW Observatories can be found from the World Data Centre for Greenhouse Gases (WDCGG): https://ds.data.jma.go.jp/gmd/wdcgg/wdcgg.html.

30   The daily passenger number data for Zugspitze were provided by Bayerische Zugspitzbahn.

References

Bader, J.: Aufbau und Betrieb eines automatisierten Gaschromatographen HP 6890 zur kontinuierlichen Messung von CO_2, CH_4, N_2O und SF_6, Universität Heidelberg, 2001.

Beardsmore, D. J. and Pearman, G. I.: Atmospheric carbon dioxide measurements in the Australian region: Data from
5   surface observatories, Tellus B, 39B, 42–66, doi:10.1111/j.1600-0889.1987.tb00269.x, 1987.

Bousquet, P., Gaudry, A., Ciais, P., Kazan, V., Monfray, P., Simmonds, P. G., Jennings, S. G., and O'Connor, T. C.: Atmospheric CO_2 concentration variations recorded at Mace Head, Ireland, from 1992 to 1994, Physics and Chemistry of the Earth, 21, 477–481, doi:10.1016/S0079-1946(97)81145-7, 1996.

Carnuth, W., Kempfer, U., and Trickl, T.: Highlights of the tropospheric lidar studies at IFU within the TOR project, Tellus
10   B, 54, 163–185, doi:10.1034/j.1600-0889.2002.00245.x, 2002.

Carnuth, W. and Trickl, T.: Transport studies with the IFU three-wavelength aerosol lidar during the VOTALP Mesolcina experiment, Atmospheric Environment, 34, 1425–1434, doi:10.1016/S1352-2310(99)00423-9, 2000.

Cerveny, R. S. and Coakley, K. J.: A weekly cycle in atmospheric carbon dioxide, Geophys. Res. Lett., 29, 967, doi:10.1029/2001GL013952, 2002.

15 Ciattaglia, L.: Interpretation of atmospheric CO_2 measurements at Mt. Cimone (Italy) related to wind data, J. Geophys. Res., 88, 1331, doi:10.1029/JC088iC02p01331, 1983.

Cleveland, R. B., Cleveland, W. S., McRae, J. E., and Terpenning, I.: STL: A seasonal-trend decomposition procedure based on loess, Journal of Official Statistics, 6, 3–73, 1990.

Cleveland, W. S., Freeny, A. E., and Graedel, T. E.: The seasonal component of atmospheric CO_2: Information from new
20   approaches to the decomposition of seasonal time series, J. Geophys. Res., 88, 10934, doi:10.1029/JC088iC15p10934, 1983.

Daniel, J. S., Portmann, R. W., Solomon, S., and Murphy, D. M.: Identifying weekly cycles in meteorological variables: The importance of an appropriate statistical analysis, J. Geophys. Res., 117, n/a-n/a, doi:10.1029/2012JD017574, 2012.

Dettinger, M. D. and Ghil, M.: Seasonal and interannual variations of atmospheric CO_2 and climate, Tellus B, 50, 1–24,
25   doi:10.1034/j.1600-0889.1998.00001.x, 1998.

Francey, R. J., Trudinger, C. M., van der Schoot, M., Krummel, P. B., Steele, L. P., and Langenfelds, R. L.: Differences between trends in atmospheric CO_2 and the reported trends in anthropogenic CO_2 emissions, Tellus B, 62, 316–328, doi:10.1111/j.1600-0889.2010.00472.x, 2010.

Frölicher, T. L., Joos, F., and Raible, C. C.: Sensitivity of atmospheric CO_2 and climate to explosive volcanic eruptions,
30   Biogeosciences, 8, 2317–2339, doi:10.5194/bg-8-2317-2011, 2011.

Frölicher, T. L., Joos, F., Raible, C. C., and Sarmiento, J. L.: Atmospheric CO_2 response to volcanic eruptions: The role of ENSO, season, and variability, Global Biogeochem. Cycles, 27, 239–251, doi:10.1002/gbc.20028, 2013.

Gantner, L., Hornsteiner, M., Egger, J., and Hartjenstein, G.: The diurnal circulation of Zugspitzplatt: Observations and modeling, metz, 12, 95–102, doi:10.1127/0941-2948/2003/0012-0095, 2003.

Gilge, S., Plass-Duelmer, C., Fricke, W., Kaiser, A., Ries, L., Buchmann, B., and Steinbacher, M.: Ozone, carbon monoxide and nitrogen oxides time series at four alpine GAW mountain stations in central Europe, Atmos. Chem. Phys., 10, 12295–12316, doi:10.5194/acp-10-12295-2010, 2010.

Hammer, S., Glatzel-Mattheier, H., Müller, L., Sabasch, M., Schmidt, M., Schmitt, S., Schönherr, C., Vogel, F., Worthy, D. E., and Levin, I.: A gas chromatographic system for high-precision quasi-continuous atmospheric measurements of CO_2, CH_4, N_2O, SF_6, CO and H_2: http://www.iup.uni-heidelberg.de/institut/forschung/groups/kk/en/GC_Hammer_25_SEP_2008.pdf, last access: 26 April 2018.

Hernández-Paniagua, I. Y., Lowry, D., Clemitshaw, K. C., Fisher, R. E., France, J. L., Lanoisellé, M., Ramonet, M., and Nisbet, E. G.: Diurnal, seasonal, and annual trends in atmospheric CO_2 at southwest London during 2000–2012: Wind sector analysis and comparison with Mace Head, Ireland, Atmospheric Environment, 105, 138–147, doi:10.1016/j.atmosenv.2015.01.021, 2015.

Huntrieser, H., Heland, J., Schlager, H., Forster, C., Stohl, A., Aufmhoff, H., Arnold, F., Scheel, H. E., Campana, M., Gilge, S., Eixmann, R., and Cooper, O. R.: Intercontinental air pollution transport from North America to Europe: Experimental evidence from airborne measurements and surface observations, J. Geophys. Res., 110, 637, doi:10.1029/2004JD005045, 2005.

Jones, C. D. and Cox, P. M.: Modeling the volcanic signal in the atmospheric CO_2 record, Global Biogeochem. Cycles, 15, 453–465, doi:10.1029/2000GB001281, 2001.

Jones, C. D. and Cox, P. M.: On the significance of atmospheric CO_2 growth rate anomalies in 2002-2003, Geophys. Res. Lett., 32, n/a-n/a, doi:10.1029/2005GL023027, 2005.

Kahle, D. and Wickham, H.: ggmap: Spatial Visualization with ggplot2, The R Journal, 5, 144–161, 2013.

Keeling, C. D., Adams, J. A., Ekdahl, C. A., and Guenther, P. R.: Atmospheric carbon dioxide variations at the South Pole, Tellus, 28, 552–564, doi:10.1111/j.2153-3490.1976.tb00702.x, 1976.

Keeling, C. D., Whorf, T. P., Wahlen, M., and van der Plichtt, J.: Interannual extremes in the rate of rise of atmospheric carbon dioxide since 1980, Nature, 375, 666–670, doi:10.1038/375666a0, 1995.

Keenan, T. F., Prentice, I. C., Canadell, J. G., Williams, C. A., Wang, H., Raupach, M., and Collatz, G. J.: Recent pause in the growth rate of atmospheric CO_2 due to enhanced terrestrial carbon uptake, Nature communications, 7, 13428, doi:10.1038/ncomms13428, 2016.

Le Quéré, C., Raupach, M. R., Canadell, J. G., Marland, G., Bopp, L., Ciais, P., Conway, T. J., Doney, S. C., Feely, R. A., Foster, P., Friedlingstein, P., Gurney, K., Houghton, R. A., House, J. I., Huntingford, C., Levy, P. E., Lomas, M. R., Majkut, J., Metzl, N., Ometto, J. P., Peters, G. P., Prentice, I. C., Randerson, J. T., Running, S. W., Sarmiento, J. L., Schuster, U., Sitch, S., Takahashi, T., Viovy, N., van der Werf, G. R., and Woodward, F. I.: Trends in the sources and sinks of carbon dioxide, Nature Geosci, 2, 831–836, doi:10.1038/ngeo689, 2009.

Lintner, B. R., Buermann, W., Koven, C. D., and Fung, I. Y.: Seasonal circulation and Mauna Loa CO_2 variability, J. Geophys. Res., 111, doi:10.1029/2005JD006535, 2006.

Liu, F., Beirle, S., Zhang, Q., Dörner, S., He, K., and Wagner, T.: NO_x lifetimes and emissions of cities and power plants in polluted background estimated by satellite observations, Atmos. Chem. Phys., 16, 5283–5298, doi:10.5194/acp-16-5283-2016, 2016.

Lucht, W., Prentice, I. C., Myneni, R. B., Sitch, S., Friedlingstein, P., Cramer, W., Bousquet, P., Buermann, W., and Smith, B.: Climatic control of the high-latitude vegetation greening trend and Pinatubo effect, Science (New York, N.Y.), 296, 1687–1689, doi:10.1126/science.1071828, 2002.

McClure, C. D., Jaffe, D. A., and Gao, H.: Carbon Dioxide in the Free Troposphere and Boundary Layer at the Mt. Bachelor Observatory, Aerosol Air Qual. Res., 16, 717–728, doi:10.4209/aaqr.2015.05.0323, 2016.

Möller, D.: Chemistry of the climate system, 2nd fully revised and extended edition, De Gruyter, Berlin, XX, 786 Seiten, 2017.

Müller, L.: Setup of a combined gas chromatographic system at the stations Schauinsland and Zugspitze for monitoring atmospheric H_2 and other greenhouse gases, University of Heidelberg, 2009.

Pales, J. C. and Keeling, C. D.: The concentration of atmospheric carbon dioxide in Hawaii, J. Geophys. Res., 70, 6053–6076, doi:10.1029/JZ070i024p06053, 1965.

Pickers, P. A. and Manning, A. C.: Investigating bias in the application of curve fitting programs to atmospheric time series, Atmos. Meas. Tech., 8, 1469–1489, doi:10.5194/amt-8-1469-2015, 2015.

R Core Team: R: A Language and Environment for Statistical Computing, Vienna, Austria: https://www.R-project.org/, 2018.

Reiter, R., Sladkovic, R., and Kanter, H.-J.: Concentration of trace gases in the lower troposphere, simultaneously recorded at neighboring mountain stations, Meteorl. Atmos. Phys., 35, 187–200, doi:10.1007/BF01041811, 1986.

Sanchez-Lorenzo, A., Laux, P., Hendricks Franssen, H.-J., Calbó, J., Vogl, S., Georgoulias, A. K., and Quaas, J.: Assessing large-scale weekly cycles in meteorological variables: A review, Atmos. Chem. Phys., 12, 5755–5771, doi:10.5194/acp-12-5755-2012, 2012.

Schmidt, M., Graul, R., Sartorius, H., and Levin, I.: The Schauinsland CO_2 record: 30 years of continental observations and their implications for the variability of the European CO_2 budget, J. Geophys. Res., 108, 535, doi:10.1029/2002JD003085, 2003.

Sirignano, C., Neubert, R. E. M., Rödenbeck, C., and Meijer, H. A. J.: Atmospheric oxygen and carbon dioxide observations from two European coastal stations 2000–2005: Continental influence, trend changes and APO climatology, Atmos. Chem. Phys., 10, 1599–1615, doi:10.5194/acp-10-1599-2010, 2010.

Slemr, F. and Scheel, H. E.: Trends in atmospheric mercury concentrations at the summit of the Wank mountain, Southern Germany, Atmospheric Environment, 32, 845–853, doi:10.1016/S1352-2310(97)00131-3, 1998.

Stephens, B. B., Brailsford, G. W., Gomez, A. J., Riedel, K., Mikaloff Fletcher, S. E., Nichol, S., and Manning, M.: Analysis of a 39-year continuous atmospheric CO_2 record from Baring Head, New Zealand, Biogeosciences, 10, 2683–2697, doi:10.5194/bg-10-2683-2013, 2013.

Sturm, P., Leuenberger, M., and Schmidt, M.: Atmospheric O_2 CO_2 and $\delta^{13}C$ observations from the remote sites Jungfraujoch, Switzerland, and Puy de Dôme, France, Geophys. Res. Lett., 32, 2467, doi:10.1029/2005GL023304, 2005.

Thoning, K. W., Tans, P. P., and Komhyr, W. D.: Atmospheric carbon dioxide at Mauna Loa Observatory: 2. Analysis of the NOAA GMCC data, 1974–1985, J. Geophys. Res., 94, 8549, doi:10.1029/JD094iD06p08549, 1989.

Trickl, T., Cooper, O. R., Eisele, H., James, P., Mücke, R., and Stohl, A.: Intercontinental transport and its influence on the ozone concentrations over central Europe: Three case studies, J. Geophys. Res., 108, 57, doi:10.1029/2002JD002735, 2003.

Trickl, T., Giehl, H., Jäger, H., and Vogelmann, H.: 35 yr of stratospheric aerosol measurements at Garmisch-Partenkirchen: From Fuego to Eyjafjallajökull, and beyond, Atmos. Chem. Phys., 13, 5205–5225, doi:10.5194/acp-13-5205-2013, 2013.

Tsutsumi, Y., Mori, K., Ikegami, M., Tashiro, T., and Tsuboi, K.: Long-term trends of greenhouse gases in regional and background events observed during 1998–2004 at Yonagunijima located to the east of the Asian continent, Atmospheric Environment, 40, 5868–5879, doi:10.1016/j.atmosenv.2006.04.036, 2006.

Ueyama, M. and Ando, T.: Diurnal, weekly, seasonal, and spatial variabilities in carbon dioxide flux in different urban landscapes in Sakai, Japan, Atmos. Chem. Phys., 16, 14727–14740, doi:10.5194/acp-16-14727-2016, 2016.

Wang, Y., Munger, J. W., Xu, S., McElroy, M. B., Hao, J., Nielsen, C. P., and Ma, H.: CO_2 and its correlation with CO at a rural site near Beijing: Implications for combustion efficiency in China, Atmos. Chem. Phys., 10, 8881–8897, doi:10.5194/acp-10-8881-2010, 2010.

Watanabe, F., Uchino, O., Joo, Y., Aono, M., Higashijima, K., Hirano, Y., Tsuboi, K., and Suda, K.: Interannual Variation of Growth Rate of Atmospheric Carbon Dioxide Concentration Observed at the JMA's Three Monitoring Stations: Large Increase in Concentration of Atmospheric Carbon Dioxide in 1998, Journal of the Meteorological Society of Japan, 78, 673–682, 2000.

Winkler, P., Lugauer, M., and Reitebuch, O.: Alpine Pumping, Promet, 32, 34–42, 2006.

WMO: Greenhouse Gas Bulletin, No. 13, 2017.

Yuan, Y., Ries, L., Petermeier, H., Steinbacher, M., Gómez-Peláez, A. J., Leuenberger, M. C., Schumacher, M., Trickl, T., Couret, C., Meinhardt, F., and Menzel, A.: Adaptive selection of diurnal minimum variation: A statistical strategy to obtain representative atmospheric CO_2 data and its application to European elevated mountain stations, Atmos. Meas. Tech., 11, 1501–1514, doi:10.5194/amt-11-1501-2018, 2018.

Zhang, F., Zhou, L., Conway, T. J., Tans, P. P., and Wang, Y.: Short-term variations of atmospheric CO_2 and dominant causes in summer and winter: Analysis of 14-year continuous observational data at Waliguan, China, Atmospheric Environment, 77, 140–148, doi:10.1016/j.atmosenv.2013.04.067, 2013.

Table 1: Detailed description of atmospheric CO_2 measurements (NDIR = Nondispersive infrared, GC = Gas chromatography, and CRDS = Cavity ring-down spectroscopy).

Site ID	Time period	Instrument (Analytical method)	Scale	Calibration gas
ZPT	1981–1997	1981–1984: Hartmann & Braun URAS 2 (NDIR)	WMO X74 scale	CO_2 in N_2
		1985–1988: Hartmann & Braun URAS 2T (NDIR)		
		1989–1997: Hartmann & Braun URAS 3G (NDIR)		
ZUG	1995–2001	Hartmann & Braun URAS 3G (NDIR)	WMO X85 scale	CO_2 in natural air
ZSF	2001–2016	2001–2016: Hewlett Packard Modified HP 6890 Chem. station (GC)	WMO X2007 scale	CO_2 in natural air
		2012–2013: Picarro EnviroSense 3000i (CRDS)		
WNK	1981–1996	Hartmann & Braun URAS 2T (NDIR)	WMO X74 scale	CO_2 in N_2

Table 2: Mean annual CO$_2$ growth rates in ppm yr^{-1} at the 0.95 confidence interval based on three time blocks. This comparison refers to data from all years including the corresponding time period for all stations. Only data for station Zugspitze from 1995–2001 are partly missing (i.e., 6-month missing data in 1998 and, thus, annual growth rates are not available for 1998 and 1999).

Time period	Schauinsland	Zugspitze	Mauna Loa	WDCGG Global	NOAA Global
1981-1994	1.45 ± 0.54	1.42 ± 0.69	1.43 ± 0.30	1.42 ± 0.36	1.40 ± 0.31
1995-2001	1.74 ± 1.11	1.49 ± 0.58	1.76 ± 0.51	1.78 ± 0.42	1.74 ± 0.45
2002-2016	2.23 ± 0.68	2.18 ± 0.40	2.19 ± 0.23	2.15 ± 0.22	2.16 ± 0.24
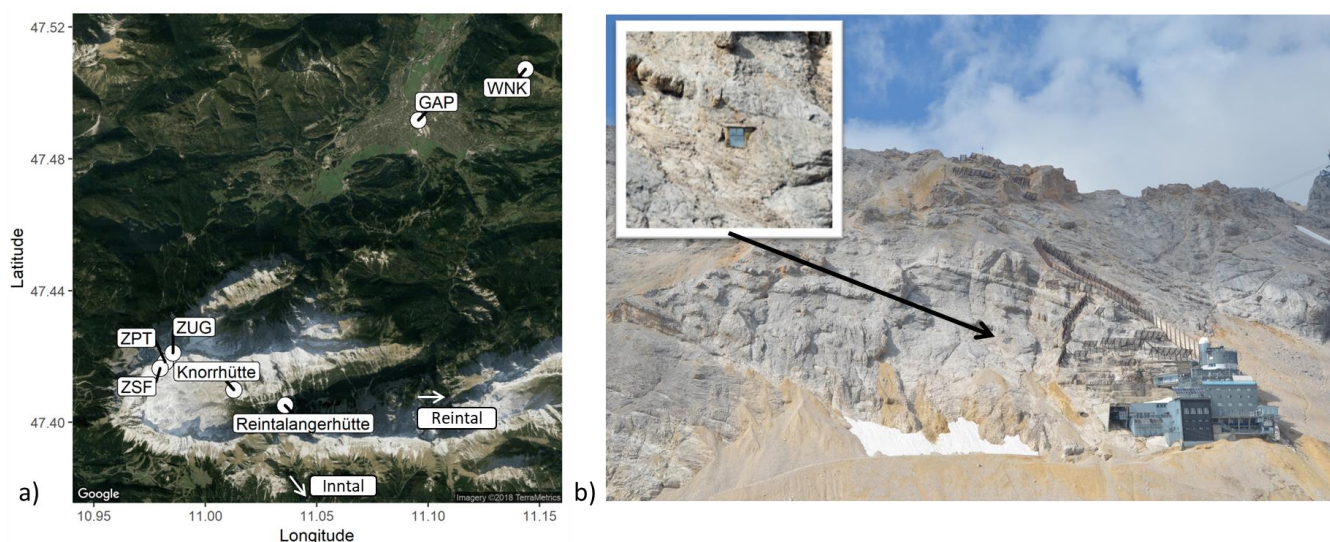
Figure 1: (a) Satellite map from Google and TerraMetrics (Kahle and Wickham, 2013) showing the study area and (b) a photograph showing the locations of the Mount Zugspitze sites in the Garmisch-Partenkirchen region (GAP) where atmospheric CO$_2$ measurements were taken. Zoomed photograph with the arrow shows the balcony for the measurement site ZPT.
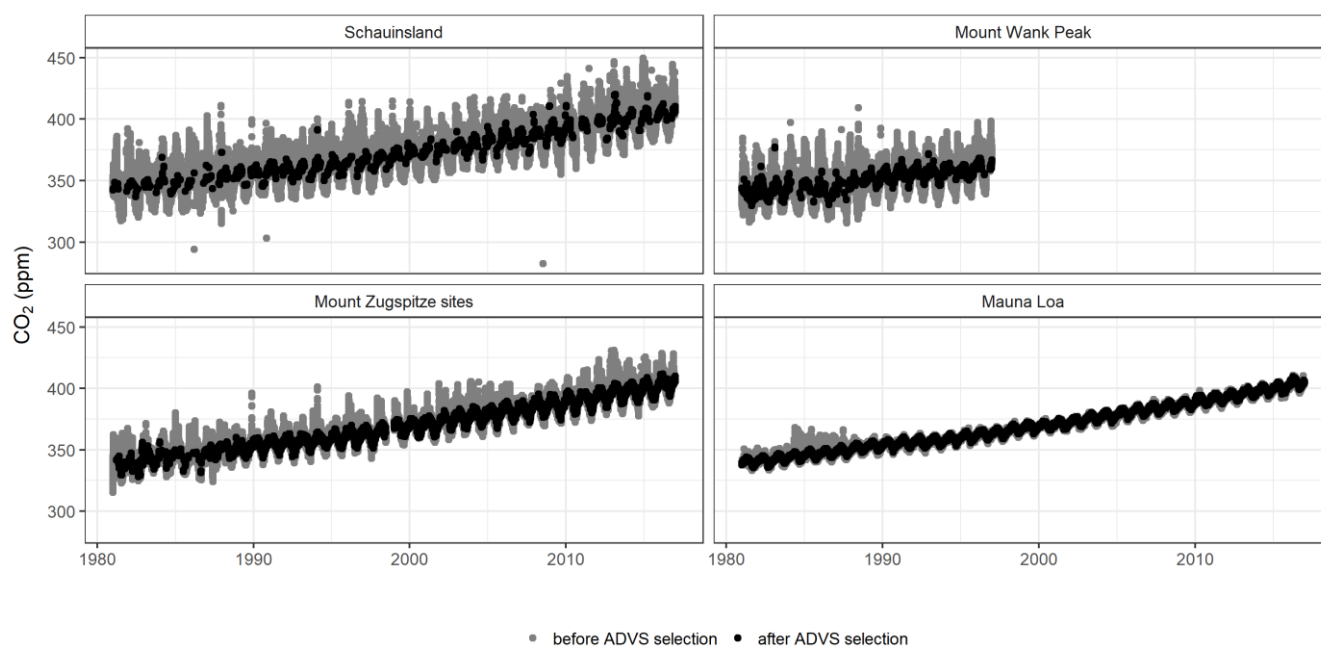
Figure 2: Time series plot of 30-min averaged CO$_2$ concentrations measured at the Wank and Zugspitze sites, and hourly averaged CO$_2$ concentrations measured at Schauinsland and Mauna Loa between 1981 and 2016 with ADVS-selected results.
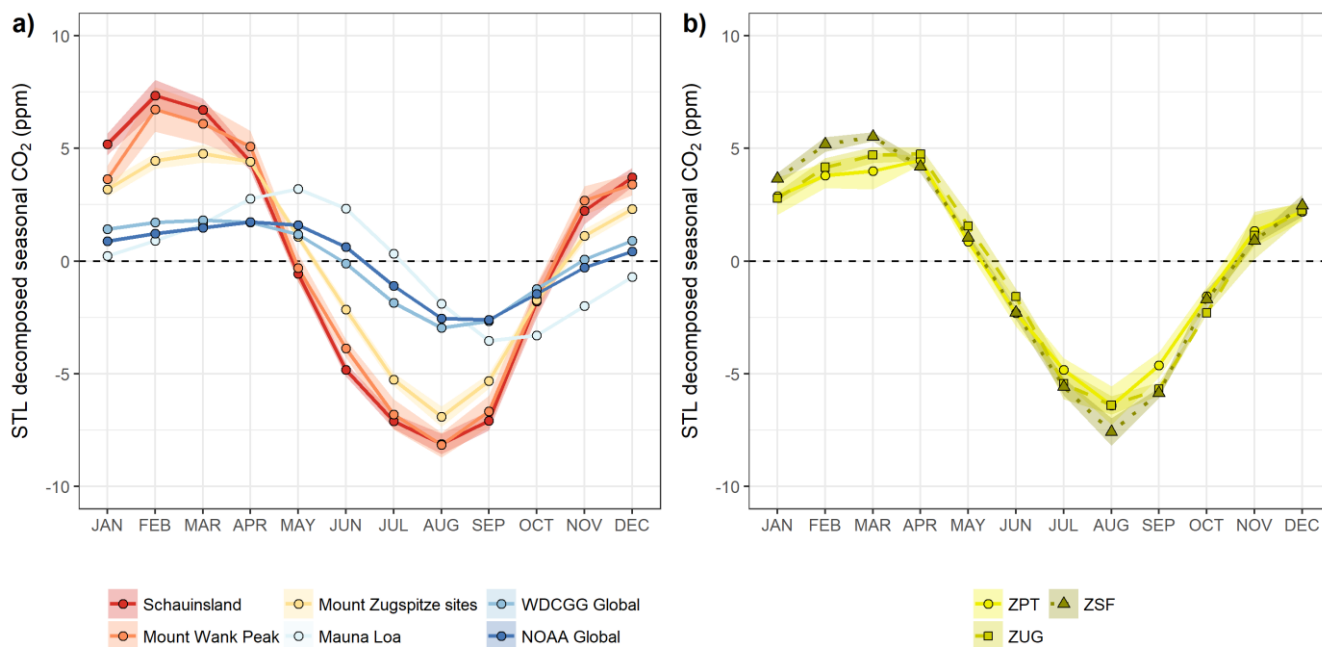
Figure 3: a) Mean CO$_2$ seasonal cycles from 1981 to 2016 (aside from WNK, which exists between 1981 and 1996). Uncertainties at a 95% confidence interval are shown by the shaded areas. b) Mean CO$_2$ seasonal cycles at ZPT (1981–1994), ZUG (1995–2001), and ZSF (2002–2016).
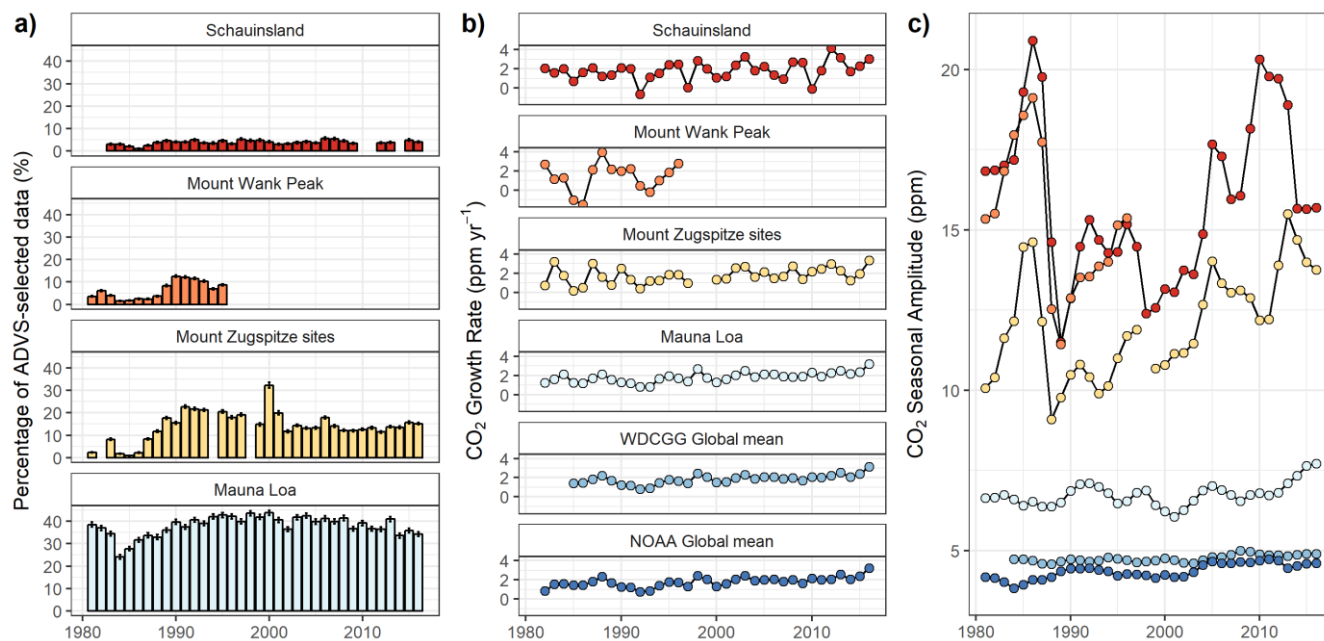
Figure 4: a) Annual ADVS-selected percentages. b) Annual CO$_2$ growth rates for all sites and global means from the NOAA and the WDCGG. The calculated growth rates are shown at the beginning of the year. Since the time period starts in 1981, the values of growth rates start in 1982. WDCGG data is only available starting 1984. c) Annual CO$_2$ seasonal amplitudes.
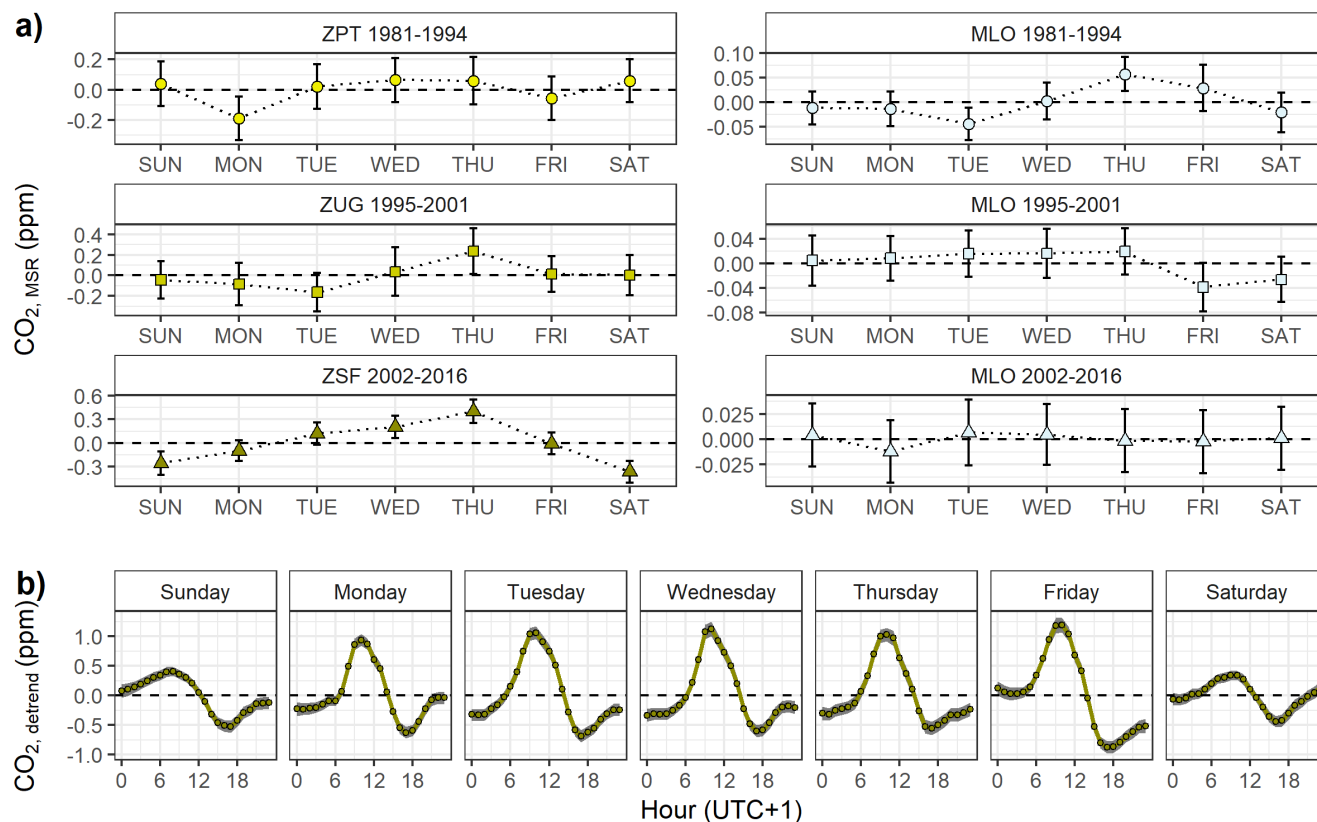
Figure 5: a) Mean MSR CO_2 values at the Mount Zugspitze sites and MLO as a function of the week day. Mean MSR values are adjusted such that they sum to 0 at each site. b) Detrended mean CO_2 diurnal cycles at ZSF by week day from 2002 to 2016. Uncertainties at a 95% confidence interval are shown by the shaded areas.
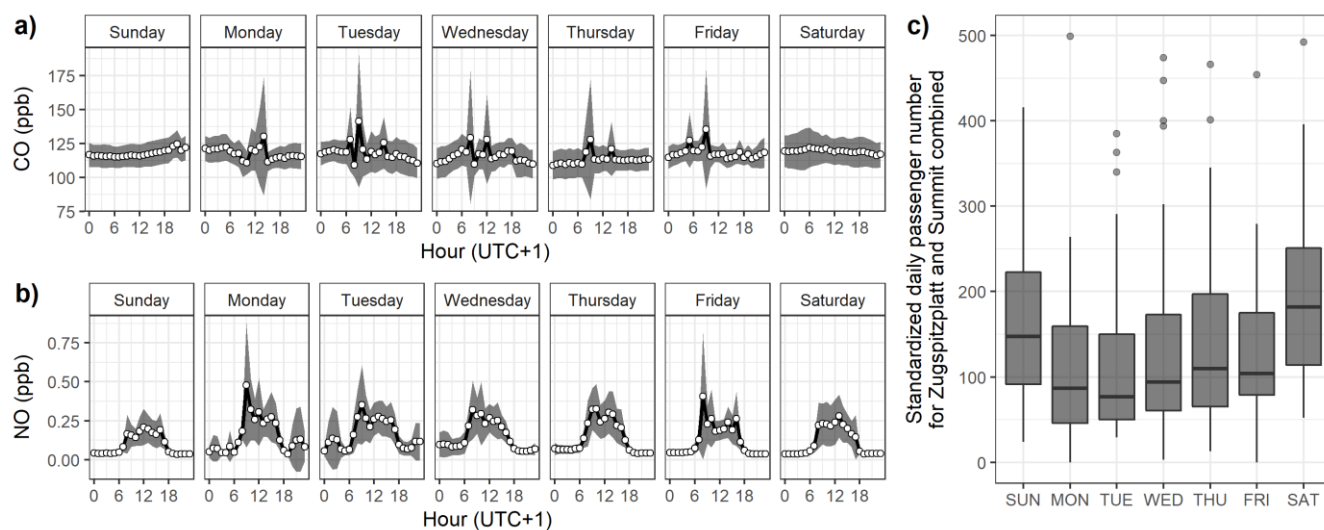
Figure 6: Mean diurnal plots at ZSF during 2016 by week day for a) CO, b) NO, and c) the standardized daily passenger number at the Zugspitzplatt and Zugspitze summit combined.